EUROPEAN FUSION DEVELOPMENT AGREEMENT

EFDA–JET–PR(04)57

W. Suttrop, V. Hynönen, T. Kurki-Suonio, P.T. Lang, M. Maraschek,
R. Neu, A. Stäbler, G.D. Conway, S. Hacquin, M. Kempenaars,
P.J. Lomas, M.F.F. Nave, R.A. Pitts, K.-D. Zastrow, the ASDEX Upgrade team
and JET EFDA contributors

Studies of the “Quiescent H-mode” Regime in ASDEX Upgrade and JET

Studies of the “Quiescent H-mode” Regime in ASDEX Upgrade and JET

W. Suttrop[1], V. Hynönen[2], T. Kurki-Suonio[2], P.T. Lang[1], M. Maraschek[1], R. Neu[1], A. Stäbler[1], G.D. Conway[1], S. Hacquin[3], M. Kempenaars[4], P.J. Lomas[5], M.F.F. Nave[3], R.A. Pitts[6], K.-D. Zastrow[5], the ASDEX Upgrade team and JET EFDA contributors*

[1]Max-Planck-Institut f¨ur Plasmaphysik, EURATOM Association, D-85748 Garching
[2]Euratom-TEKES Association, Helsinki University of Technology, P.O. Box 2200, FIN-02015 HUT, Finland
[3]Associac¸òao EURATOM/IST, Centro de Fusòao Nuclear, Instituto Superior T´ecnico, 1049-001 Lisboa, Portugal
[4]FOM-Instituut for Plasmaphysica ìRijnhuizenî, Association EURATOM-FOM, P.O. Box 1207, 3430 Nieuwegein, The Netherlands
[5]Euratom/UKAEA Fusion Association, Culham Science Centre, Abingdon, Oxfordshire, OX14 3DB, UK
[6]Association Euratom-CRPP, Ecole Polytechnique F´ed´erale de Lausanne, 1015 Ecublens, Switzerland
** See annex of J. Pamela et al, “Overview of Recent JET Results and Future Perspectives”, Fusion Energy 2002 (Proc.19 th IAEA Fusion Energy Conference, Lyon (2002).*

Preprint of Paper to be submitted for publication in
Nuclear Fusion

ABSTRACT

The stationary ELM-free "Quiescent H-mode" (QH-mode) regime, obtained with counter neutral beam injection, is studied in ASDEX Upgrade and JET. QH-mode plasmas have high pedestal and core ion temperatures together with good H-mode con nement. ELMs are replaced by continuous MHD oscillations, the "Edge Harmonic Oscillation" (EHO) and the "High Frequency Oscillation". Stationarity of particle and impurity densities is linked to the occurrence of these MHD modes. The EHO location in the steep-gradient region and its appearance with increasing edge pressure points at the edge pressure or pressure gradient as possible drivers for the EHO. Injection of small cryogenic pellets can raise the plasma density to about 40% of the Greenwald density limit without triggering ELMs. Orbit-following calculations of the slowing down distribution show the presence of an enhanced fast particle density in the H-mode barrier region despite the large loss currents with counter-injection. The radial electrical field in the edge barrier region, about twice as large in QH-mode compared to ELMy H-mode, is large enough to reverse the precession drift direction of injected beam ions, leading to a resonance of the EHO with the drift precession frequency.

1. INTRODUCTION

The "High-confinement" mode (H-mode) is considered a reliable regime for achieving adequate fusion yield in the planned ITER experiment and in a nuclear fusion reactor. However, at the large temperature and pressure values on top of the edge transport barrier (the H-mode "pedestal"), type I Edge Localised Modes ("ELMs") are usually obtained. If the ablation thresholds for both metal and graphite divertors are exceeded [1], type I ELMs may impose unacceptable peak heat loads on the divertor target in a large scale fusion device.

Therefore, con nement regimes that allow for large pedestal pressure in order to maintain good confinement, but with small or no ELMs are needed to prevent excessive erosion and migration of divertor material inside the tokamak vessel.

Usually, particle transport across the H-mode barrier occurs mainly during ELMs, so that ELM-free H-modes are typically characterised by accumulation of density and impurities, terminated by a large ELM or thermal collapse. The "Quiescent" H-mode (QH-mode) regime, recently discovered in DIII-D [2] is ELM-free, but with stationary density and impurity content. At the same time, the con nement is comparable to or better than in a typical type-I ELMy H-mode. The QH-mode regime has been reproduced and studied in ASDEX Upgrade [3]. Meanwhile, H-mode behaviour similar to that of a QH-mode has been found in JT-60U [4].

Here we report further studies of QH-mode properties in ASDEX Upgrade and experiments to scale up the QH-mode regime to larger plasmas in the Joint European Torus (JET). The next two sections summarise the conditions and phenomenology of the QH-mode in both machines. Subsequently, we describe the properties of the MHD behaviour that replaces ELMs in QH-mode and discuss the possible reasons for the suppression of ELMs in this regime.

2. PHENOMENOLOGY OF QH-MODE IN ASDEX UPGRADE

So far in ASDEX Upgrade, QH-mode has been only seen with counter-current neutral beam injection (counter-NBI). In agreement with experience in DIII-D [2], large plasma-wall clearance (in ASDEX Upgrade typically 8cm gap in the main chamber), good pumping (using the lower divertor cryopump), and low neutral gas pressure appear helpful in obtaining long stationary QH-mode phases. The experiments have been carried out with a plasma current of I_p = 1MA and a toroidal field B_t between 2.0 and 2.5T (q_{95} = 3.6...4.5).

Fig.1 shows time traces of two pulses that enter QH-mode: No:17686 with a mixture of 2 semi-tangential NBI sources (one at E = 60keV beam energy with tangency radius R_{tan} = 0.93m and one at E = 93keV with R_{tan} 0.84m), and No: 17694 with two radial sources (E = 60keV with R_{tan} 0.53m). The plasma con guration and total NBI heating power are identical. The transition to QH-mode occurs earlier and the QH-mode phases are longer with more tangential injection, in line with observations at DIII-D [5]. Note that with more tangential injection the plasma density remains constant or drops after the transition to QH-mode, while with radial injection both edge and core densities, after an initial drop, increase to levels above those in ELMy H-mode before the transition. A transition to QHmode is also obtained with the pair of tangential NBI sources installed at ASDEX Upgrade (E = 93keV with R_{tan} 1.29m, on the high field side), but the density quickly drops below the minimum density to avoid NBI shine-through. Note that while radial and semi-tangential sources produce trapped particles in a wide radial range, the tangential sources produce mostly passing particles inside the plasma, and a significant trapped particle fraction only near the H-mode pedestal. In ASDEX Upgrade, QH-mode has been obtained at various levels of effective ion charge Z_{eff}, the lowest value obtained so far being Z_{eff} = 2.5[6]. ELMy and QH-mode phases with counter injection show similar values of Z_{eff}.

3. QH-MODE EXPERIMENTS IN JET

During the 2003 reversed plasma current campaign in JET, dedicated experiments were carried out to identify the QH-mode regime in plasmas of larger size. The con guration used (shown in the insert in Fig. 3) combines large wall clearance (15cm outboard and inboard gaps) and good exhaust by positioning the strike points for optimum cryo-pumping in the Mark II SRP Gasbox divertor. Low recycling conditions are obtained by a combination of He glow discharge cleaning followed by a lengthy period of cryo-pumping and beryllium evaporation in the main chamber. Discharges are heated with up to 14MW of counter current neutral beams. Different combinations of plasma current and magnetic field are used: 2.5MA/ 2.7T (q_{95} = 3.3), 1.7MA/ 2.15T (q_{95} = 4.9), 1.7MA/ 2.25T (q_{95} = 4.3) and 1.5MA/ 2.2T (q_{95} = 4.7).

In these discharges, extended ELM-free phases with up to 1.5s duration are found. Fig. 2 shows Pulse No: 59611 (I_p = 2.5MA, B_t 2.7T, q_{95} = 3.3) with type I ELMs until t = 17.2s, followed by an ELM-free phase until 18.6s. During the ELM-free time interval, radiated power (top panel) and electron density (third panel) remain stationary, indicating that the particle con nement time is not

drastically increasing in the absence of ELMs. This behaviour is as expected for QH-mode and is in contrast to the increases in density and radiation usually found in traditional ELM-free phases. As is often seen in the smaller machines with counter-injection at low density, Z_{eff} is high, ranging between 4 and 5 in JET, independent of the presence of ELMs. Con nement is at or above the H98y scaling, and no deterioration during the ELM-free phase is seen. These stationary ELM-free phases are accompanied by the characteristic Edge Harmonic Oscillation (EHO), which is observed both in magnetic measurements and in X-mode reflectometry measurements with cut-off layer in the H-mode barrier region. We therefore identify these phases as transitions to the QH-mode regime in JET. In addition, pronounced core MHD behaviour is observed in most discharges. While the cases with q_{95} = 3.3 have sawteeth, the plasmas at higher q ($q_{95} \geq 4$) generally show n = 1, m = 1 fishbone activity.

In Fig. 3, core temperature and density pro les of an ELMy and a QH-mode phase are compared in the same discharge. The ECE and charge exchange spectroscopy measurements (edge and core systems) indicate that there is little difference in electron and ion temperatures through most of the pro le and at the H-mode pedestal top. Also, as shown by core LIDAR measurements, the plasma density is similar in the two regimes.

Although the observed ELM-free phases show many of the features characteristic of the QH regime, it has not been possible in JET to reproduce the same behaviour in repetitive pulses with identical parameters or to produce extended QH-mode periods for longer than about 1.5s or three con nement times. It appears that the longest quiescent phases occur in plasmas produced immediately after the wall conditioning cycles or following repeated low recycling discharges with high NBI power and minimum external gas input.

4. MHD ACTIVITY IN QH-MODE

QH-mode pulses usually show rich MHD activity. In the plasma core, shbone or continuous m = 1, n = 1 oscillations prevail at higher edge safety factor, whilst at low q, sawtooth oscillations occur. A range of discharges has no discernible m = 1, n = 1 activity.

4.1. THE "EDGE HARMONIC OSCILLATION"

The most pronounced MHD feature of the QH-mode is that ELMs are replaced by the characteristic "Edge Harmonic Oscillation" (EHO, [2]). The name originates from the many harmonics observed in spectrograms of magnetic measurements. In ASDEX Upgrade and JET, the EHO fundamental has so far always been found at a toroidal mode number n = 1. Electron cyclotron emission (ECE) and radially deconvoluted Soft X-ray measurements in ASDEX Upgrade as well as microwave re ectometer data in JET show that the EHO is located in the H-mode edge transport barrier region. Figure 4 (bottom trace) shows a spectrogram measured with the JET KG8b X-mode reflectometer during a quiescent phase in JET Pulse No: 59611. The probing frequency of 76GHz corresponds to a cut-off position in the gradient region. The double-sided frequency spectrum from heterodyne detection (in-phase and quadrature signals) shows an oscillation with a fundamental frequency of about 15kHz and up to six harmonics (bright colours correspond to high intensity). The spectrum is

symmetric, as expected for the radial launching direction of the re ectometer antennas. The middle trace represents the total intensity of the reflectometer signal, which is varying little during the quiescent phase. There are uctuations of the D_α intensity (top trace), which are correlated with the EHO frequency as seen in the re ectometer. For instance, in the time interval from $t = 22.05$ to $t = 22.07$s the D_α intensity increases by about 50% while the EHO fundamental frequency drops from 15kHz to about 11kHz (the frequencies of its harmonics drop accordingly).

A safety factor scan in ASDEX Upgrade shows that the poloidal mode number adjusts itself such that the EHO remains localised on a flux surface in the gradient region [6]. The ECE measurement also reveals that the perturbations outside and inside the rational surface are in phase, as would be expected for a kink mode, and not in the case of a magnetic island.

Magnetic measurements at different toroidal locations show practically identical waveforms, phase shifted according to the toroidal angle of the measurement as expected for an $n = 1$ mode. This suggests that the EHO is a rigidly rotating mode, i.e., the harmonic spectrum originates from its spatial structure, not from a time-dependent perturbation in the rotating frame.

Figure 5 shows the EHO waveform as seen by a radial field pick-up coil in ASDEX Upgrade (measuring dB_r/dt) which is located 10cm from the separatrix at the outer midplane (upper trace). The raw signal is smoothed by a comb filter set to pass the EHO fundamental and its harmonics and reject noise at other frequencies. The ltered signal is integrated, resulting in a signal proportional to B_r (middle trace). For a kink-like perturbation the radial field B_r is proportional to the spatial derivative $d\xi/dl$ along a field line. Thus, for a rotating mode, the time integral of B_r gives a signal which is proportional to ξ as a function of toroidal angle. This signal is shown in the bottom trace. The sharp minima and maxima of the raw magnetic signal, which give rise to the pronounced harmonic spectrum of the EHO, correspond to regions of large curvature near the minima and maxima of ξ. The EHO waveform can be described as near triangular.

4.2. THE "HIGH FREQUENCY OSCILLATION"

In addition to the EHO, an MHD oscillation at high frequencies occurs in ASDEX Upgrade [3], typically between 300 and 450kHz and with a toroidal mode number of $n = 5$. Often, an additional higher frequency signal (not at an integer multiple frequency) is observed. The HFO amplitude is modulated in time (seen as characteristic bursts) as shown in Fig. 6 which compares a high-pass filtered fast B_r signal (middle trace) with the EHO (taken here from a peripheral Soft X-ray chord and a slow magnetic signal with bandpass lter at the EHO frequency and its harmonics). The HFO envelope, with a toroidal $n = 0$ structure, has the same frequency and a fixed phase relationship with the EHO cycles for each toroidal location.

4.3. TRANSPORT ASSOCIATED WITH EDGE MHD ACTIVITY

The absence of ELMs in H-mode usually causes a large increase of the particle confinementtime, typically leading to an accumulation of deuterium and impurities, often terminated by an unusually large ELM or a thermal collapse of the plasma. In contrast, the density and radiation in QH-mode

are quite stationary. One may ask whether the pronounced edge MHD causes or at least contributes to particle and energy loss across the separatrix. Indeed, the HFO bursts and EHO cycles are strongly correlated with the outer divertor D_α intensity [3]. The inner divertor D_α signal shows no correlation. The D_α time lag of about 20μs [3] is consistent with the transit time of ions at 10keV energy to the divertor, i.e. typical for ions lost from the neutral beam slowing down distribution. If there are losses of thermal particles, they are overwhelmed by this signal.

Indirect evidence of thermal particle and heat losses associated with edge MHD in QHmode comes from other observations. Figure 7 shows time traces of ASDEX Upgrade shot 18931, in which four pellets have been injected into a QH-mode plasma. The first three pellets result in a moderate but clearly visible increase of the core density. After the fourth pellet (at t = 3.26s), the amplitude of the magnetic signal B_r drops and after this time the central and peripheral line densities are no longer stationary but continue to rise until several ELMs occur. Figure 8 shows a spectrogram of the magnetic signal that demonstrates the presence of the EHO before and in between pellet injection times and its disappearance after the last pellet is injected. We note that the disappearance of the EHO marks the loss of QH-mode and density control.

With counter neutral beam injection, the EHO is often visible in ELMy phases as well, as shown in Fig. 9. The ELM times are identified by the spikes in the divertor D_α signal. During the ELM cycle, the EHO (from measured B_r in between ELMs) appears only shortly before an ELM. The edge line density and pedestal-top electron temperature (second panel) drop due to the particle and energy losses associated with each ELM, but recover rapidly within the first half of the inter-ELM cycle. Thereafter, they remain almost saturated until the next ELM occurs. The product of these signals is indicative of the pedestal top pressure, which shows the same temporal behaviour. The onset of the EHO in each cycle coincides with the beginning of the pressure saturation.

Since the heat flux from the plasma interior is continuous, this temporal behaviour suggests that with the onset of the EHO heat transport across the edge barrier increases. In addition, the disappearance of the EHO after each ELM and its onset at the time the pressure recovers suggests that the pressure or edge pressure gradient in the barrier region plays a role in driving the EHO.

In order to study impurity transport across the H-mode barrier, silicon is injected into a QH-mode plasma by laser-blow-off from a solid target (Fig. 10). The silicon content in the plasma core is monitored by a flat crystal Bragg spectrometer that measures the intensity of a Si XIII (He-like) line at a wavelength of 0.665nm. After the short injection pulse at t = 2.59s, the intensity drops with a time constant of several hundred milliseconds, despite the increasing electron density. This time scale is similar to that determined in Ref. [7] for Si in ELMy H-mode plasmas with co-injection. We conclude that there is measurable impurity transport across the barrier in QH-mode.

5. FAST PARTICLE EFFECTS

5.1. FAST PARTICLE DISTRIBUTION IN THE BARRIER REGION

In QH-mode, a strong enhancement of the charge exchange neutral particle flux at high particle energies is observed [3]. Since the density of recycling neutrals in QH-mode is at or below that in

ELMy H-mode, the enhancement of the charge exchange flux indicates a strong increase of the fast ion population at the plasma edge. The neutral beam slowing-down distribution is simulated using the Monte Carlo based particle following code ASCOT [8]. The magnetic equilibrium as well as the plasma temperature and density profiles are extracted from the ASDEX Upgrade QH-mode Pulse No: 17695 at t = 5.6s. Two NBI sources (E = 60keV, R_{tan} = 0.93m) produce a flux of Γ_{NBI} 7.3×10^{20} particles/second. The ionisation profiles for full, half and third energy components of the beam are calculated by the FAFNER code [9]. From the initial ion distribution (birth position, energy and pitch angle), a set of 10^5 test particles is generated, and the slowing down is followed in ASCOT down to twice the thermal velocity. Orbits that intersect the limiter are counted as losses; the radial flux due to these loss orbits is recorded as a function of radius. For counter-injection, the region for significant loss current is found to extend into the plasma down to a normalised poloidal flux radius ρ_p = 0 7. The four-dimensional distribution function is recorded as the total time spent in slots of ρ_p, poloidal angle, total velocity v_{tot} and pitch $v_{||}/v$. In a given phase space volume, the total number of actual plasma particles is the total time spent by test particles, multiplied by the ratio of particle source rate to number of test particles. Thus summing over all test particles during the simulation corresponds to steady-state injection. Fig.11 shows contour plots of a section of the fast particle distribution (time spent in seconds) as a function of radius ρ_p and total velocity v_{tot} for Pulse No:17695 (a), and for the corresponding co-injection case, obtained by reversing the initial pitch angles in the simulation (b).

For counter injection (Fig.11(a)), the maximum fast particle density extends further outward (to about ρ_p = 0.93) than for its co-injection counterpart (ρ_p = 0.85, Fig.11(b)). With the given beam geometry, almost all particles ionised near the H-mode pedestal top are trapped. Because of the outward-opening orbits in counter-injection there is a significant number of particles automatically aligned so that their orbits extend into the edge barrier region and, hence, to the resonant flux surface of the EHO. This population exists despite strong orbit losses from the plasma edge.

5.2. REVERSAL OF THE PRECESSION DRIFT DIRECTION

Fast particles can interact with modes in different ways, the effect can be stabilising by finite Larmor radius stabilisation, or de-stabilising if a resonance between the particle motion (bounce frequency or toroidal drift precession frequency) occurs. For the magnetic field configuration used in the present counter-injection experiments, in the absence of a radial electrical field the toroidal drift precession is directed opposite to the injection direction. In contrast, both the EHO and HFO rotate in the injection direction (the electron drift direction when projected to the plane perpendicular to the magnetic field).

However, a sufficiently large inward-directed radial electrical field E_r not only affects the magnitude of the precession drift frequency but can also reverse the direction of the precession drift. Experimentally, it is observed that the peak E_r in the H-mode barrier region for a fully established QH-mode is significantly larger than for an ELMy H-mode. This is measured, independently, by

Doppler re ectometry in ASDEX Upgrade [10] and, using radial force balance, from charge exchange spectroscopy in DIII-D [5]. A peak E_r of about 60kV/m is found in ASDEX Upgrade QH-modes [10].

We consider the orbit of a typical ion representing the semi-tangential beam in ASDEX Upgrade. Such an ion is injected at an energy of 60keV and has a pitch angle $v_{||}/v$ of 0.45 at the outboard midplane. Figure 12 shows the effect of a homogeneous radial electrical field on the drift precession frequency of particles with $v_{||}/v$ of 0.45 born at different radii ρ_p, as calculated with ASCOT. In the absence of a radial electrical field the toroidal precession frequency ω_{prec} is about −60... −70krad/s. The critical radial electrical field for reversing the direction of the toroidal precession from clockwise (as viewed from above the torus) to counter-clockwise is about −25kV/m, a value which is exceeded in QH-mode in the pedestal region. Due to the shape of the *q* profile, ions born at smaller radii have higher positive precession frequencies. For E_r 60kV/m, a maximum of ω_{prec} =110krad/s is reached. This frequency exceeds the rotation frequency of the EHO (*f* 7 11kHz, corresponding to wEHO 44 69 krad/s). While the precession drift frequency is strongly affected by *E*r, the bounce frequency changes very little (within about 10%).

We conclude that it is possible that a resonance between injected fast ions and the EHO occurs. Since the ASCOT calculations reveal the existence of strong gradients (in real space and velocity space) aligned with the H-mode barrier region, we can also speculate that fast ions from counter-NBI play a role in driving the EHO. In this picture a balance between the fast particle drive of the EHO and increasing fast particle losses with increasing EHO amplitude could account for the stationarity of the mode amplitude. An analog observation of an edge MHD mode which is destabilised by fast particles might be the "outer mode", a continuous *n* 1 kink mode found in JET D-T discharges [11], which appears as the alphaparticle population slowly restores after giant ELM events.

5.3. NARROWING OF ION ORBITS

A radial electrical field affects the width of fast particle orbits that intersect a region of significant *E*r. With negative *E*r, as is found in the H-mode barrier region, counter-injected trapped ions lose kinetic energy as they follow their drift orbits that take them radially outward. As a consequence, the radial width of their drift orbits is smaller than with zero or positive E_r. For co-injected particles the orbits widen for $E_r < 0$ and shrink for $E_r > 0$. This effect of a radially inward-directed electrical field of constant magnitude is illustrated in Fig. 13, which shows the orbits of co-injected and counter-injected ions with 60keV energy, born at $\rho_p = 0.7$, for $E_r = -20$keV (solid lines), compared with the case $E_r = 0$ (dashed lines). In addition, an inhomogenous electrical field can either shrink ($dE_r/d_r < 0$) or widen ($dE_r / d_r > 0$) the trapped orbits, an effect that is independent of the injection direction. This effect is called "orbit squeezing", [12] in the case of a negative gradient.

The narrowing of the orbits also affects the fast particle density at the edge. For the experimental situation discussed above, and with $E_r = 0$, only ions born inside $\rho_p = 0.77$ have drift orbits that remain entirely inside the separatrix. A negative (inward directed) E_r reduces the orbit width and, thus, increases the number of ions in the pedestal region. The experimentally observed E_r profile is

modelled here with a simple square well for a semi-quantitative picture. With E_r = 20kV/m inside ρ_p = 0.9 and E_r 60kV/m for ρ_p = 0.9...1.0, it is found that even ions born at ρ_p = 0.81 will remain inside the main plasma. Consequently, a higher fast ion density can build up in the H-mode barrier region in presence of a negative radial electrical field such as that observed in QH-mode.

6. SUMMARY AND CONCLUSIONS

The quiescent H-mode regime combines stationary good con nement, high pedestal pressure, and low pedestal collisionality ($\nu^* < 1$) with the absence of ELMs. So far, QH-mode is obtained only with counter-neutral beam injection. Good pumping conditions, achieved e.g. by placing the strike points in a position for good divertor pumping, seem to facilitate access to QH-mode. However, it is not yet possible to quantify the access conditions for QH-mode. Longest QH-mode phases in ASDEX Upgrade (ELM-free for the entire heating phase) and JET (ELM-free for about 1.5s) have been found after fresh vessel conditioning, but it is difficult to say whether the change in the recycling conditions or suppression of impurity in flux is in uencing QH-mode access. High Z_{eff} is often found with counter injection, but it is not necessarily an essential property of QH-mode. The impurity mix in QH-mode and ELMy phases with counter-NBI is quite similar and depends more on the machine conditions than on the presence or absence of ELMs. Edge transport in QH-mode seems to be linked with the occurrence of the Edge Harmonic Oscillation and the High Frequency Oscillation, which are always seen in QH-mode phases, and sometimes also in between ELMs. So far, the EHO is observed only with counter-NBI in ASDEX Upgrade. It is also unclear whether QH-mode discharges can be fuelled up to densities near the Greenwald limit. Gas puffing usually leads to a rapid transition to ELMy H-mode. First experiments with pellet fuelling show that pellets do not trigger ELMs in a QH-mode as they usually do in ELMy H-modes with co-NBI [13].

So far, the density increase is limited to about 40% of the Greenwald density. The QH-mode density limit is marked by disappearance of the EHO and a transition to a non-stationary phase terminated by ELMs.

A related, interesting question is what causes the suppression of ELMs in QH-mode. The main observations are as follows:

1. The edge current and pedestal top pressure in the barrier are not reduced compared to ELMy H-mode. This is likely to be true of the current density and pressure gradient as well.
2. In fully established QH-mode, the E_r well in the edge barrier region is significantly deeper than in ELMy H-mode.
3. A significant population of trapped high-energy particles exists at the plasma edge, self-aligned with the H-mode barrier region due to ionisation in the high-density core and extending into the edge because of the outward pointing drift orbits associated with counter-NBI.

The first observation implies that reaching the same edge pressure gradient and the same edge current density as just before ELMs is not suf cient to generate an ELM event. The latter two

observations point at a possible suppression of ELMs either by strong $E \times B$ velocity shear or by finite Larmor radius stabilisation by fast particles. These possibilities require further experimental and theoretical investigation.

ACKNOWLEDGEMENT

The authors would like to thank S. G¨unter for valuable discussions and CSC, the Finnish IT centre for science, Espoo, Finland (www.csc.fi) for providing the resources to run the ASCOT code.

REFERENCES

[1]. G. Federici, P. Andrew, P. Barabaschi, J. Brooks, R. Dörner, A. Geier, A. Herrmann, G. Janeschitz, K. Krieger, A. Kukushkin, et al., J. Nucl. Mater. 313-316 (2003) **11**.

[2]. K.H. Burrell, M.E. Austin, D.E. Brennan, J.C. DeBoo, E.J. Doyle, P. Gohil, C.M. Greenfield, R.J. Groebner, L.L. Lao, T.C. Luce, et al., Plasma Phys. Controlled Fusion **44** (2002) A253.

[3]. W. Suttrop, M. Maraschek, G.D. Conway, H.-U. Fahrbach, G. Haas, L.D. Horton, T. Kurki-Suonio, C.J. Lasnier, A.W. Leonard, C.F. Maggi, et al., Plasma Phys. Controlled Fusion **45** (2003) 1399.

[4]. Y. Sakamoto, H. Shirai, T. Fujita, S. Ide, T. Takizuka, N. Oyama, and Y. Kamada, Plasma Phys. Controlled Fusion **46** (2004) 299.

[5]. K.H. Burrell, W.P. West, E.J. Doyle, M.E. Austin, J.S. deGrassie, P. Gohil, C.M. Greenfield, R.J. Groebner, R. Jayakumar, D.H. Kaplan, et al., Plasma Phys. Controlled Fusion **46** (2004) 165.

[6]. W. Suttrop, G.D. Conway, L. Fattorini, L.D. Horton, T. Kurki-Suonio, C.F. Maggi, M. Maraschek, H. Meister, R. Neu, T. Pütterich, et al., Plasma Phys. Controlled Fusion **46** (2004) A151.

[7]. R. Dux, R. Neu, A.G. Peeters, G. Pereverzev, A. Mück, F. Ryter, J. Stober, and ASDEX Upgrade Team, Plasma Phys. Controlled Fusion **45** (2003) 1815.

[8]. J.A. Heikkinen,W. Herrmann, and T. Kurki-Suonio, Plasma Phys. **4** (1997) 3655.

[9]. G.G. Lister, Technical Report 4/222, IPP, Garching, Germany, 1985.

[10]. G.D. Conway, J. Schirmer, S. Klenge, W. Suttrop, E. Holzhauer, and ASDEX Upgrade Team, Plasma Phys. Controlled Fusion **46** (2004) 951.

[11]. G.A. Cottrell, V.P. Bhatnagar, O. Da Costa, R.O. Dendy, J. Jacquinot, K.G. McClements, D.C. McCune, M.F.F. Nave, P. Smeulders, and D.F.H. Start, Nucl. Fusion **33** (1993) 1365.

[12]. R.D. Hazeltine, Phys. Fluids B 1 (1989) 2031.

[13]. P.T. Lang, G.D. Conway, T. Eich, L. Fattorini, O. Gruber, S. Günter, L. D. Horton, S. Kalvin, A. Kallenbach, M. Kaufmann, et al., Nucl. Fusion **44** (2004) 665.

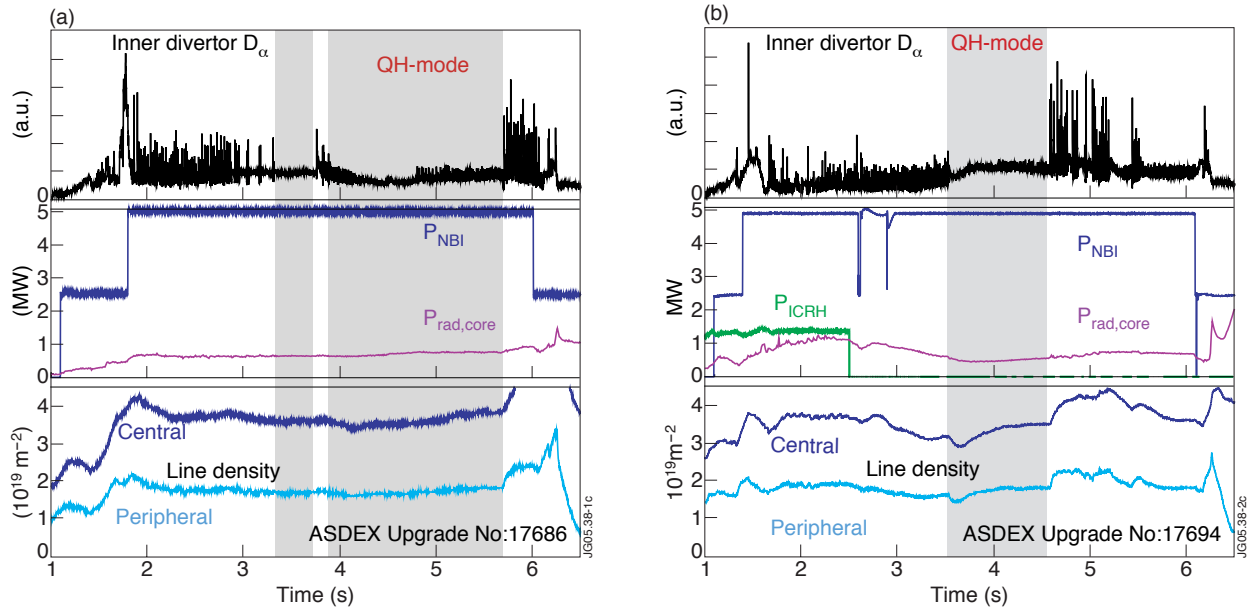

Figure 1: Time traces of QH-mode discharges in ASDEX Upgrade with semi-tangential and radial NBI sources.

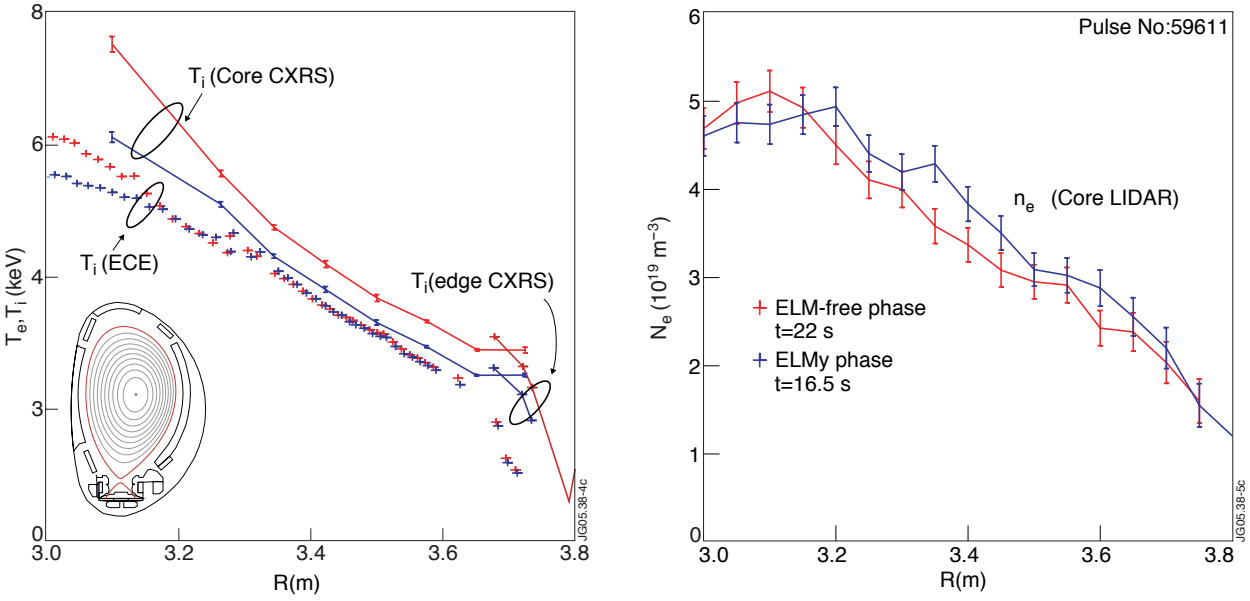

Figure 2: Time traces of JET Pulse No: 59611 with an extended QH-mode phase.

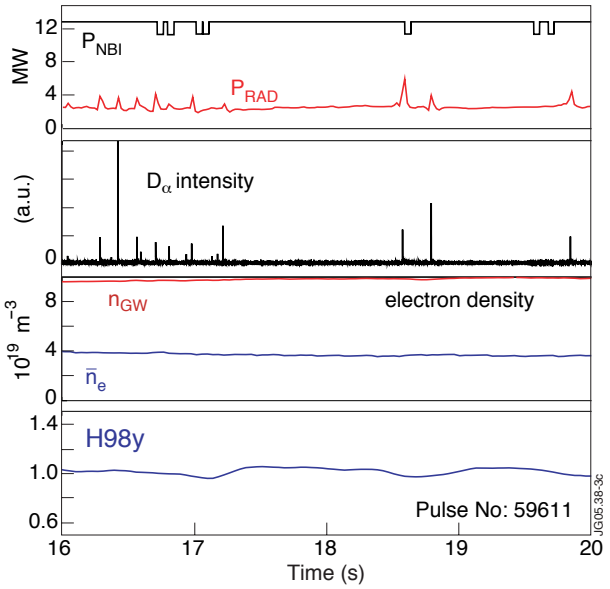

Figure 3: Temperature and density profiles in ELMy and QH phases of JET Pulse No:59611.

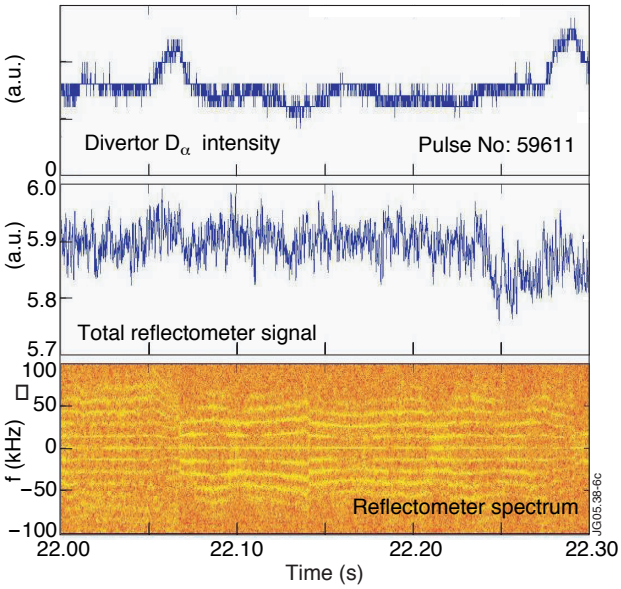

Figure 4: Observation of the EHO in JET with fixed frequency X-mode reflectometry.

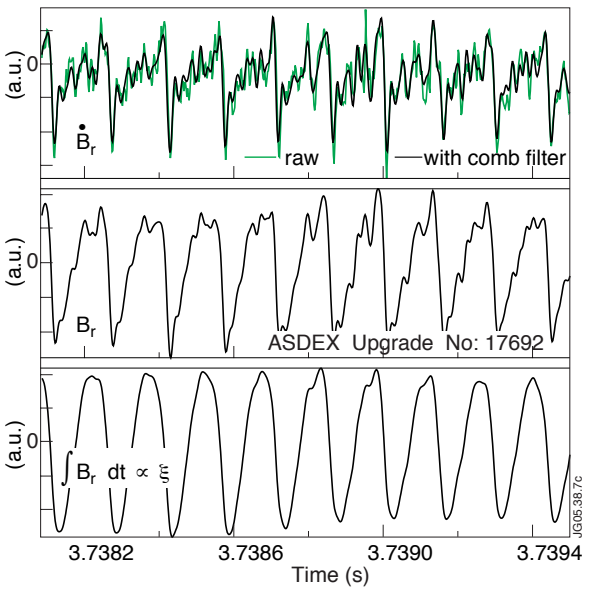

Figure 5: EHO signal of ASDEX Upgrade Pulse No: 17692 measured by a magnetic probe and integrated twice, yielding a signal proportional to the radial displacement ξ.

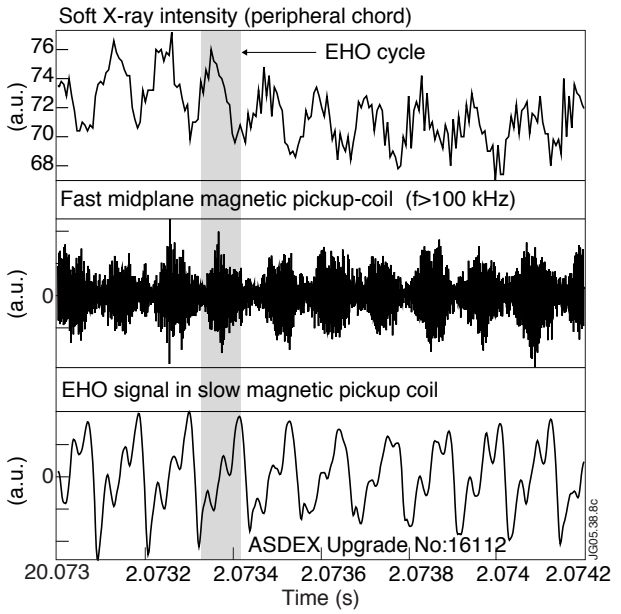

Figure 6: "High frequency oscillation" (HFO) and the temporal relation of HFO bursts with EHO cycles as seen in Soft X-ray and magnetic measurements.

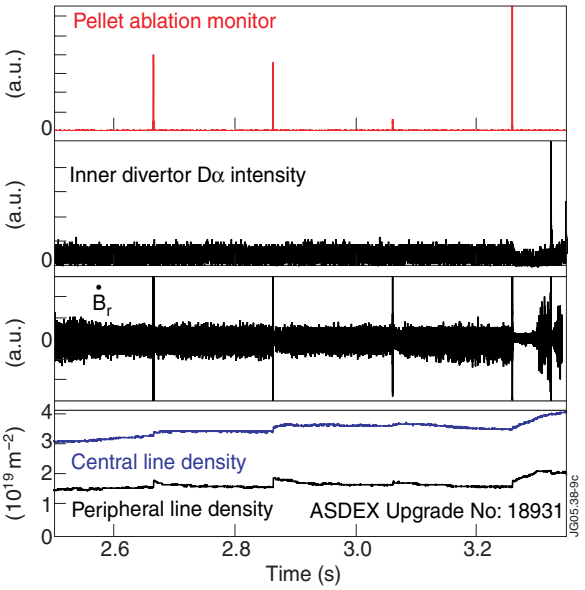

Figure 7: Pellet injection in QH-mode in ASDEX Upgrade.

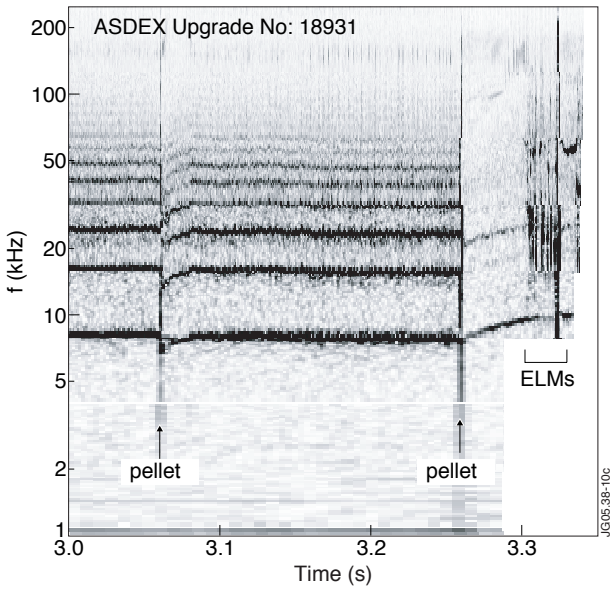

Figure 8: Spectrogram of the Mirnov coil signal showing the EHO and its disappearance after the last pellet of the shot shown in Fig. 7.

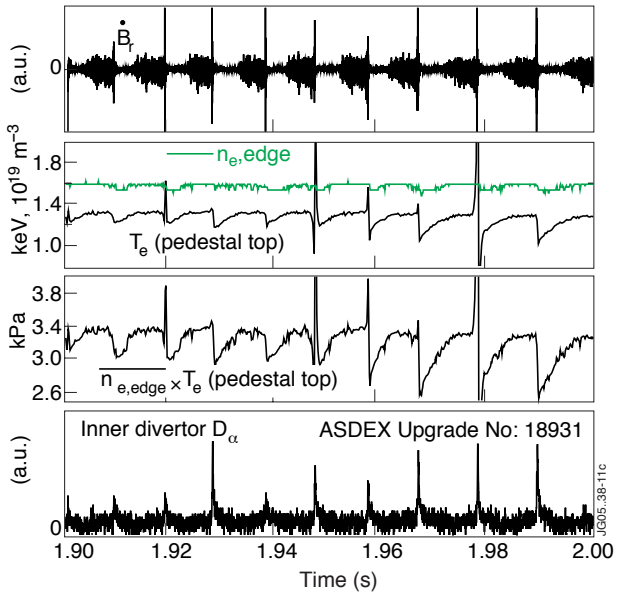

Figure 9: ELMy phase in a shot with counter-NBI. In between ELMs, the EHO appears as the edge pressure approaches its maximum. With EHO present, the pressure saturates.

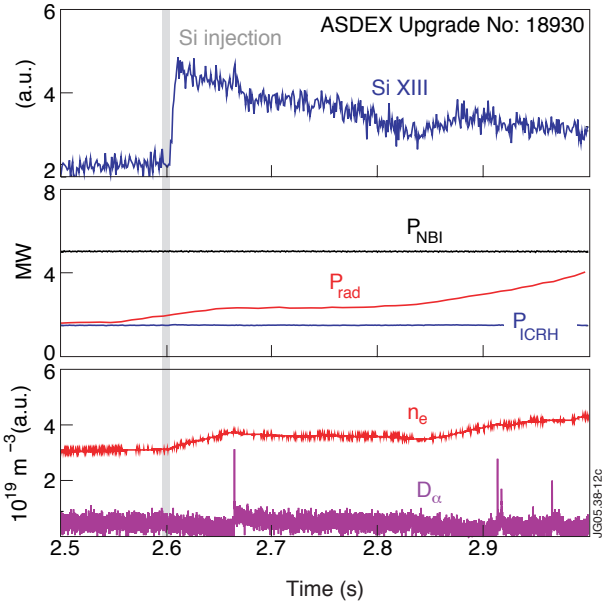

Figure 10: Impurity (Si) injection, monitored spectroscopically by Si XIII emission.

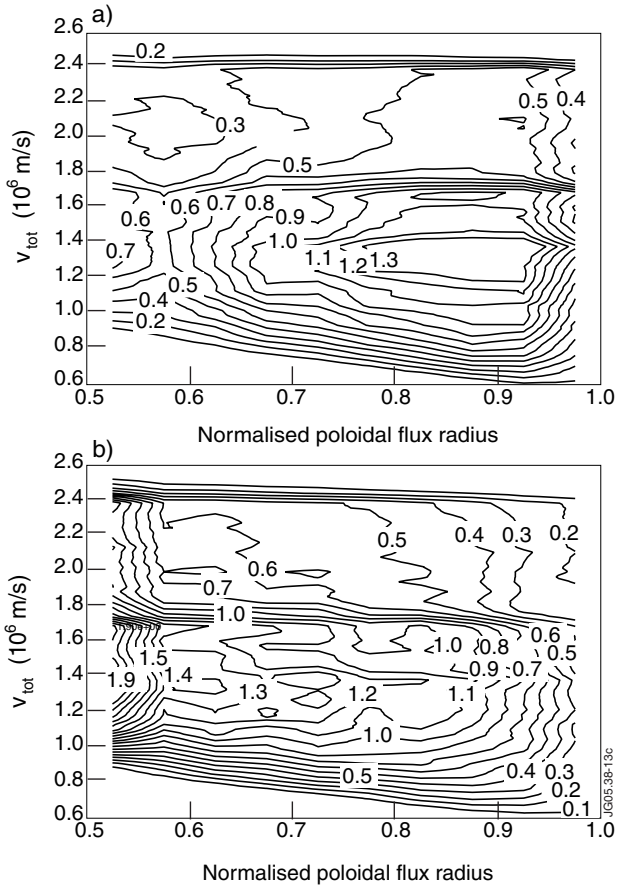

Figure 11: Fast particle distribution calculated with ASCOT for counter-injection and for coinjection with identical background plasma.

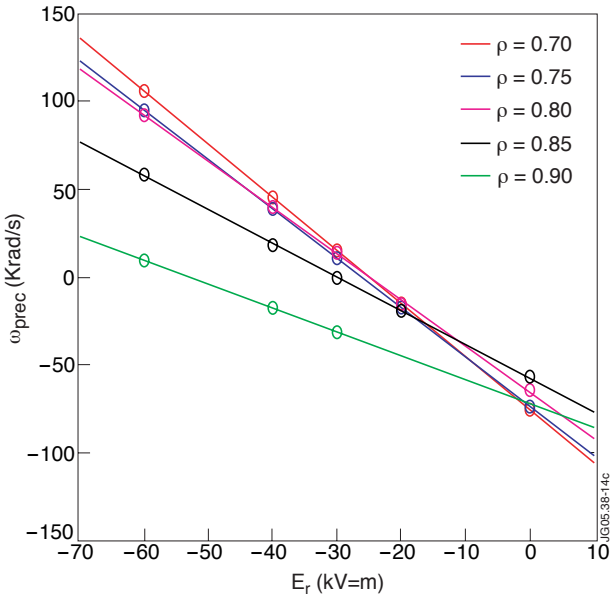

Figure 12: Effect of a spatially constant radial electrical field on the precession drift frequency for different birth radii.

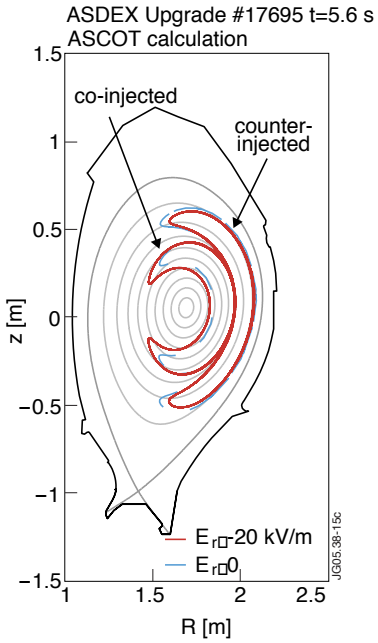

Figure 13: Orbits of co- and counter-injected ions born at $\rho_p = 0.7$ in presence of a radially inward-directed electrical field of constant magnitude ($E_r = -20$ keV) and $E_r = 0$.